

Heat dissipation from stationary passenger car brake discs

Stergios Topouris¹ – Dragan Stamenković^{2*} – Michel Olphe-Galliard¹ – Vladimir Popović² - Marko Tirović¹

¹ Cranfield University, School of Aerospace, Transport and Manufacturing, Cranfield, UK

² University of Belgrade, Faculty of Mechanical Engineering, Belgrade, Serbia

The paper presents experimental investigation of the heat dissipation from stationary brake discs concentrated on four disc designs, a ventilated disc with radial vanes, two types of ventilated discs with curved vanes - a non-drilled and cross-drilled disc, and a solid disc. The experiments were conducted on a purpose built Thermal Spin Rig and provided repeatable and accurate temperature measurement and reliable prediction of the total, convective and radiative heat dissipation coefficients. The values obtained compare favourably with Computational Fluid Dynamics results for the ventilated disc with radial vanes and solid disc, though the differences were somewhat pronounced for the ventilated disc. The speeds of the hot air rising above the disc are under 1 m/s, hence too low to experimentally validate. However, the use of a smoke generator and suitable probe was very useful in qualitatively validating the flow patterns for all four disc designs. Convective heat transfer coefficients increase with temperature but the values are very low, typically between 3 and 5 W/m²K for the disc designs and temperature range analysed. As expected, from the four designs studied, the disc with radial vanes has highest convective heat dissipation coefficient and the solid disc the lowest, being about 30% inferior. Convective heat dissipation coefficient for the discs with curved vanes was about 20% lower than for the disc with radial vanes, with the cross drilled design showing marginal improvement at higher temperatures.

Keywords: brake disc, heat dissipation, convective cooling, computational fluid dynamics, natural convection

Highlights:

- Heat dissipation from stationary brake discs was investigated.
- It was done through Thermal Spin Rig test, CFD analysis and smoke generator test.
- Radial vanes provide highest convective heat dissipation coefficient and solid disc the lowest, with curved vanes being in the middle.
- Cross drilled design shows only marginal improvement.

0 BACKGROUND

Brake cooling is vital for safe vehicle operation and has attracted substantial research from very early days, however most research and published data relate to heat dissipation from rotating discs. Cooling of a stationary brake is equally important as many critical cases are related to this driving condition. For instance, brake fluid is much more likely to boil if the vehicle is not moving. The consequences can only become apparent once the vehicle starts moving again, making the situation safety critical. Convective heat dissipation is drastically reduced, from predominantly forced cooling (at high air speeds) to natural convection only (air speed being zero). Instead of the heat being dissipated to the surrounding air, which is propelled away from the brake, much more heat is being transmitted to pads and caliper through conduction and radiation.

Furthermore, considerable portion of the heat being dissipated from the disc by natural convection is heating the caliper as the hot air is forced upwards by the natural convection. The air surrounding the brake assembly is 'trapped' within the wheel and wheel arch cavities and the brake ambient temperature is rapidly increasing, well above the outside ambient air temperature.

The situation might be equally critical during 'hot parking', when the vehicle is parked after heavy brake use. In such conditions some brake components can reach higher temperatures than for a moving vehicle. Traditionally, the risks with 'hot parking' were related to boiling of brake fluid, however vehicle 'roll away' is another potentially critical condition. As the disc and pads cool down they 'shrink' (their thickness reduces) whereas the caliper expands as it heats up as a result of a heat transferred from the pads and disc. This leads to the reduction of the clamp force,

*Corr. Author's Address: University of Belgrade, Faculty of Mechanical Engineering, Kraljice Marije 16, Belgrade, Serbia,
dstamenkovic@mas.bg.ac.rs

causing decrease in friction force (braking torque) and potentially leading to rollaway if the vehicle is parked on a gradient. The condition is most critical when installing Electric Parking Brake (EPB) where long flexible cables are not used and there is no flexibility in the system to compensate for reduction in disc and pad thickness. EPB has brought hot parking to an entirely new level, ensuring safe vehicle parking on a gradient (being specified at 20% by UN Regulation No. 13H). The methodologies used to cope with this challenge include 'over-clamping' (i.e. applying much higher force than required in order to 'stretch' the caliper which should compensate for disc and pad shrinkage) and re-parking (i.e. re-applying the brake automatically after the vehicle has been parked).

With the installation of electric and electronic components into calipers (EPB, 'low drag' calipers etc.), there is a potential danger with overheating and permanent damage to these parts, hence accurate prediction of brake temperature in parking conditions is becoming even more important.

Heat dissipation from stationary brake is also important for accurately predicting brake temperatures in drive cycles which contain periods when the vehicle is stationary. Though these cycles are typically not safety critical from the brake performance point of view, brake temperatures are important in understanding and minimising residual drag, providing good brake pedal feel and reliably estimating brake wear.

Finally, braking of Hybrid and electric vehicles (HEVs) imposes another braking challenge, in addition to complexities related to brake pedal feel, residual drag and EPB. The UN Regulation No. 13H require all braking tests (such as repeated brake applications – 'fade and recovery') to be successfully performed by friction brakes only, without the use of regenerative braking. Considering HEVs are typically heavier than equivalent cars with internal combustion engines only, understanding braking requirements is paramount not only regarding safety but also in order to minimize brake mass and resolve brake cooling in the most effective way for both moving and stationary vehicle operation. Though some of these vehicles are relatively low performance, there are some extremely high performance HEVs with very rapid acceleration characteristics and therefore very high braking demands.

When analysing brake thermal aspects in parking conditions, it should be pointed out that critical cooling times can be quite prolonged, for passenger cars with 'classical' hand brake designs, the rollaway are known to have occurred up to 30 minutes after the vehicle was parked with hot brakes. This was for 'medium gradients' (~10%) as for the higher gradients the rollaway occurs much quicker. In commercial vehicles, the critical period can be up to 1 hour [1].

As a first step in studying heat dissipation from stationary passenger car disc brake assemblies, the focus will be on the brake disc. Four types of brake discs will be studied, for two passenger vehicles. The first vehicle is Volkswagen Passat (Typ 3C) and the second Lotus Elise S2, with the basic vehicle and disc characteristics given in Table 1.

Table 1. Vehicle characteristics

Characteristic	VW Passat 2.0T FSI 2007	Lotus Elise S2 2011
Gross vehicle mass [kg]	2100	1141
Static front axle load [kg]	1080	570.5
Static rear axle load [kg]	1020	570.5
Wheelbase [mm]	2709	2300
Maximum engine power [kW]	147	89*
Maximum vehicle speed [km/h]	235	205
Front disc type	Ventilated with radial vanes	Ventilated with curved vanes**
Front disc outer diameter [mm]	321	288***
Rear disc type	Solid	Ventilated with curved vanes**
Rear disc outer diameter [mm]	286	288***

* Basic model

** Option: Cross drilled

*** Front and rear discs are identical

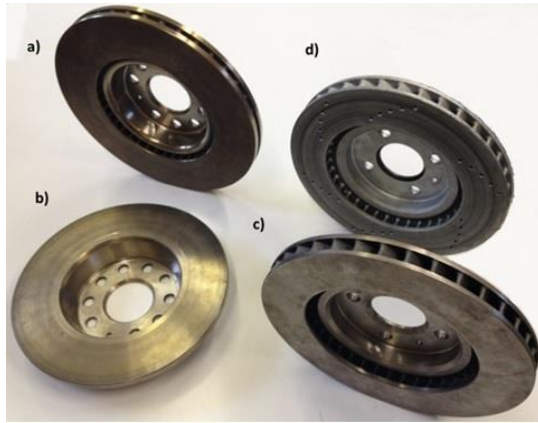


Fig. 1. Discs Analysed - VW Passat: (a) front, (b) rear Lotus Elise S2: (c) standard, (d) cross drilled

Table 2. Disc characteristics

Ref. Fig. 1	Type / Design	OD x ID x thick. [mm]	No. of vanes [-]	Wetted area [m ²]	Mass [kg]
a)	Ventilated with radial vanes	321 x 188 x 25	40	0.3086	9.4
b)	Solid	286 x 180 x 12	N/A	0.1678	3.2
c)	Ventilated with curved vanes	288 x 185 x 26	37	0.2562	4.2
d)	Ventilated with curved vanes, cross drilled	288 x 185 x 26	37	0.2586	4.18

Brake discs are shown in Fig. 1, with (a) and (b) presenting VW Passat front and rear discs respectively. Lotus Elise S2 standard disc is marked (c) in Fig. 1, with (d) presenting a cross drilled disc (the perspective of the photo can confuse the reader leading him to percept Lotus discs as unequal in diameter). From Fig. 1 it can be noted that all three ventilated discs are of a 'swan neck' type, meaning that the outboard disc friction face is attached to the top hat section but using a 'swan neck' type feature in order to minimise disc coning. This design allows air intake from the inboard side, resulting in good cooling characteristics.

Detailed design characteristics for all four discs studied are presented in Table 2. At the beginning of the research all discs were brand new. In order to stabilise emissivity values they were

repeatedly heated and cooled which caused all surfaces to corrode. Front VW Passat disc (a) is the largest and heaviest, owing the high vehicle mass and maximum speed, as well as brake force distribution (Front:Rear) of 2.1 for fully laden vehicle. Solid disc (b) has smallest outer (OD) and inner (ID) diameters, it is thinnest, has smallest wetted area and is also lightest at only 3.2 kg. It is worth pointing out that both vehicles have practically 50:50 static load distribution for fully laden condition. Whereas this substantially changes for unladen state of VW Passat (with much more load taken by the front axle in unladen and partly laden conditions), there is practically no difference for Lotus Elise as the engine is mounted in the middle and in addition to the driver, there is only place for one passenger (next to the driver) and very little luggage. Consequently, neither the load nor the distribution per axle change much for Lotus. Without entering into further analyses into brake sizing and characteristics, a brief literature review will be presented, which will be followed by the modelling and experimental results obtained.

1 LITERATURE REVIEW

Due to its importance for safe vehicle operation, heat dissipation attracted considerable research from the early days. However, complex geometry, installation, boundary conditions and service duties limited the application of analytical methods and the work was predominantly experimental, aiming at measuring maximum brake temperatures at specific duties. The research was also mostly concerned with rotating discs, with analytical methods applied initially to a geometrically perfect disc shape (not an actual brake disc) rotating in still air [2], and in a cross flow [3,4]. Heat dissipation was experimentally investigated in the past for brake discs installed on vehicle [5,6] or inertia dynamometer [7], with the aim of establishing relationships and finding effective solutions in predicting brake disc temperatures. The ability to model the actual brake geometry came with the development of numerical methods (Finite Element and Finite Difference) but the complexity of boundary conditions still required substantial experimental work in establishing and validating temperature prediction procedures. Substantial contributions to solving the problem can be found in the literature [8-11].

The development of Computational Fluid Dynamics (CFD) made possible for actual boundary conditions, i.e. convective heat transfer coefficients to be reliably theoretically predicted. Still, it took some time for these methods to be sufficiently developed for successful analyses of brake discs. Complex geometry, boundary conditions and disc rotation required robust algorithms and very powerful computers to deal with models having millions of cells. Stationary disc analysis was not any easier to model. The disc does not rotate but the energy for air flow is provided by change in air density due to its heating and expansion. Some useful CFD work for rotating disc analysis and optimisation for automotive and railway discs is provided in the literature [12-16].

There are only a few papers published and known to the authors dealing with CFD modelling in predicting temperatures and heat transfer coefficients for a stationary disc [1,17,18], and are results of studies conducted at Cranfield University. The conclusions are multifold but can be summarised in that effective CFD modelling of the stationary discs is possible nonetheless it requires meshes with a large number of elements and extreme care in their creation (in particular when modelling boundary layers). Obviously, powerful computers are needed and CPU times are considerable (typically over 48 hours). Menter's Shear Stress Transport (SST) turbulence model was found to be the most suitable in terms of both accuracy and speed. The values of convective heat transfer coefficients are similar but higher than the values quoted in this paper. This is due to much larger discs (outer diameter being 434 mm) heated to higher temperatures (over 350°C). It was also concluded that flow patterns change with temperatures and static disc cooling at higher temperatures can be reduced by the hot air exiting lower ventilation channels and blocking air entry into upper channels. This phenomenon was typical for large anti-coning type discs studied but some evidence of similar effects has been also detected by the authors and will be presented and discussed later. The analyses [1] also employed analytical methods for heat transfer from surfaces (walls and cylinders), developed by other authors [19-22]. Very useful results have been obtained for a wide temperature range, but these are limited to solid discs only.

Convective heat dissipation prediction in friction brakes has been vastly improved in recent

years nonetheless still considerably relies on experimental work. This is not limited to this mode of heat dissipation only, but also to radiative and conductive losses. Both these modes are speed independent and the radiation is highly temperature dependent. Consequently, appropriate modelling of these two modes is vital for accurate prediction of convective losses and brake temperatures in any operating duty. Substantial work and contribution in effectively tackling these modes can be found in the literature, for conductive heat transfer [23,24] as well as for radiation [25,26]. Accurate and reliable heat dissipation is required not only for safe prediction of brake temperatures regarding friction characteristics (fade) and brake components and fluid temperatures – it has much wider implications in lightweight designs and NVH (noise, vibration and harshness) characteristics [27,28].

2 EXPERIMENTAL SET-UP

All tests presented in this paper were conducted on a specially designed Thermal Spin Rig, with its CAD model shown in Fig. 2. The Rig has an in-line arrangement of the motor, coupling, drive shaft and brake disc, with suitable bearing housing placed on a supporting frame/table. Fig. 3 shows the actual Rig. In order to minimise conductive heat losses, contact areas of the disc with the mounting flange were insulated using low conductivity temperature resistant gasket (showing green in Fig. 3a). Furthermore, only 2 bolts were used to secure the disc and tightening torque was very low. The bolt contacts with the flange was also insulated by using PTFE tape (seen white in Fig. 3a). Interestingly, there was no measurable difference in cooling rates if the insulation was not placed between contact surfaces. The explanation is that both heating and cooling periods were long and if no insulation was used, the flange was heated to the same temperature and cooled down at similar rate.

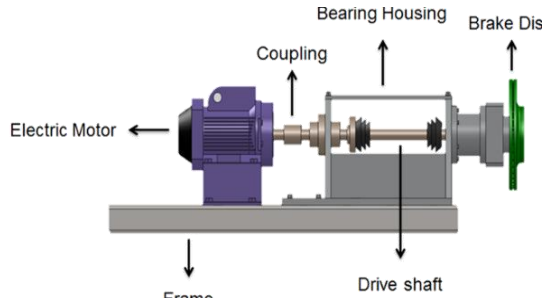


Fig. 2. Thermal Spin Rig concept

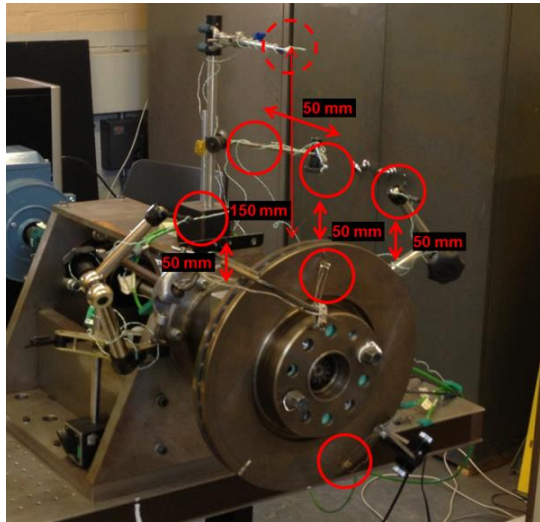


Fig. 3a. Thermal Spin Rig - thermocouples installed

The operational procedure has three distinctive phases:

a) **Heating period** - The disc is rotating at low speed (~ 100 rpm) and the heater box is placed over the disc (see Fig. 3b) with hot air guns activated, providing a gradual, uniform disc heating. Once the disc reaches the required temperature, typically around 250°C , the heating is turned off, with the disc continuing to rotate at low speed. Temperatures and other variables are logged during this period but typically not processed.

b) **Soaking period** - The disc is continuing to rotate at low speed for several minutes in order to equalise the temperatures. All variables are logged during this period for monitoring purpose but not typically processed. At the end of this period the heating box is removed.

c) **Cooling down period** - This period starts after the soaking period and all variables are logged and processed during this period. The disc is typically cooled down to under 50°C . Disc surface temperatures logged during this period make the

actual 'cooling curves' and are used to calculate average heat transfer coefficients.



Fig. 3b. Thermal Spin Rig - heating box

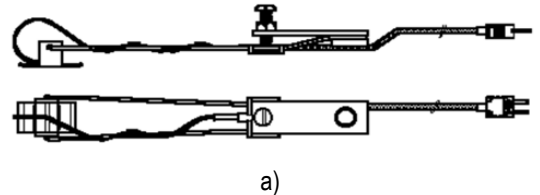
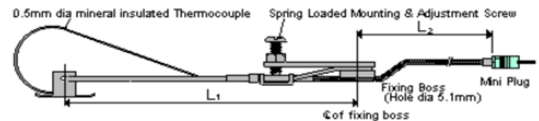
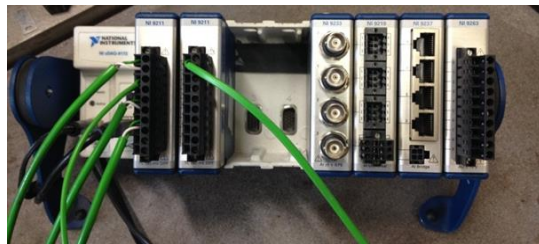


Fig. 4. Thermocouples used: (a) Rubbing/Contact thermocouple and (b) Wire thermocouple

The instrumentation used (see Fig. 3a) consisted of a number of rubbing/contact thermocouples (Fig. 4a, K Type, supplied by TC

Direct) which were positioned around the disc, contacting disc friction surfaces. It should be pointed out that differences in measured disc temperatures across friction surfaces were very small. This is a result of low cooling rate and thick disc faces made of thermally highly conductive grey cast iron. Fig. 3a shows two contact thermocouples positioned 30 mm radially from the disc outer diameter, on the bottom and top of the outboard friction face. Two more thermocouples were placed at the same nominal position on the inboard friction surface. Temperature of the air in the plume above the disc was measured using 5 thermocouples, positioned above the disc, as shown in Fig. 3a, using wire type thermocouples (Fig. 4b, also K Type). Ambient temperature was measured in 4 places around the laboratory and all doors and windows were closed to reduce air movement.



a)



b)

Fig. 5. National Instruments equipment: (a) CompactDAQ and (b) Thermocouple Module

For signal conditioning and data logging, National Instruments CompactDAQ was used (Fig. 5a) connected to a PC, together with NI 9211 thermocouple modules (Fig. 5b). The developed code enabled direct temperature measurement and display during the cooling period, as well as presentation of the entire cooling event, as shown in Fig. 6. It can be noticed that all temperatures are very close and the cooling curves are smooth. Consequently, the temperatures can be suitably

averaged and reliably used to calculate average heat transfer coefficients. The tests were repeated numerous times and nearly identical values were obtained. More details about the methodology, uncertainty and the results are available in [1,29].

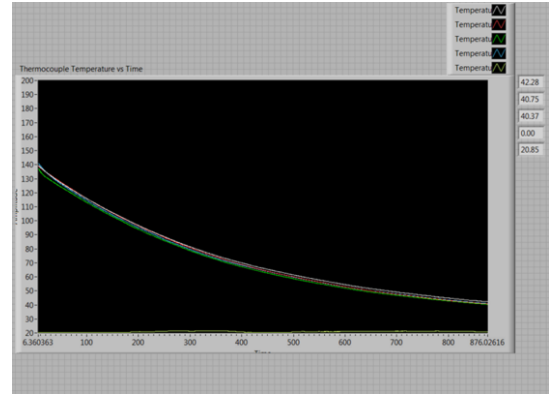
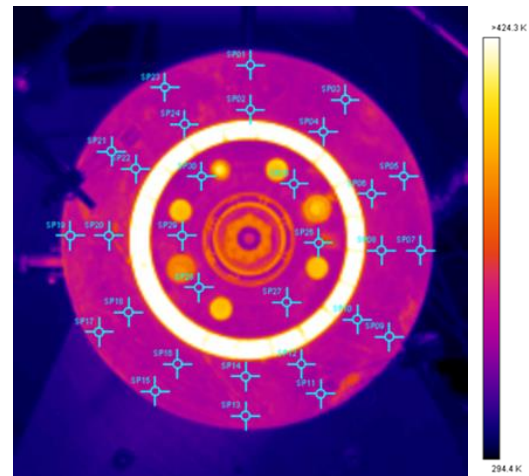


Fig. 6. Cooling curves obtained using contact (rubbing) thermocouples



(a)



(b)

Fig. 7. Infrared temperature measurements: (a) FLIR A320 Camera and (b) full field disc thermal image and selected points

In order to try and obtain more temperature data across the friction face and hub flange area of

the disc, thermal imaging camera FLIR A320 was also used (Fig. 7a), with Fig. 7b showing the image and selected points for obtaining temperatures at selected points. Unfortunately, this was not providing useful results, as minor differences in disc surface condition lead to small differences in emissivity values, which in turn caused differences in obtained temperature readings. The differences were typically around 5°C, but sometimes higher – even 10°C or more, without any reason for the difference (except change in emissivity) and with contact thermocouples showing identical temperatures in these areas. Still the cooling curves were smooth and averaging was possible. However, such differences in local temperatures were typically reducing but not diminishing as disc was cooling down and even existed when the disc was approaching or reaching ambient temperature. Though the use of infrared camera for temperature measurements of fast rotating discs at high temperature was found useful by some authors and recently much improved [26], for the considered disc, the temperature range and stationary cooling condition, this method was not considered suitable.

In order to compare the results with Computational Fluid Dynamics (CFD) predictions, an attempt was made to measure air temperatures of the plume above the disc, using wire thermocouples shown in Fig. 4b, with the positions marked in Fig. 3a. Unfortunately, this approach was found to be unsuitable. The temperature variations were irregular ('erratic'), despite every effort in preventing air movement in the laboratory. It is interesting to point out that this method was found reliable, but for much larger and heavier discs, heated to higher temperatures [1].

The problems with better understanding stationary disc cooling is not related to temperature measurements only. As it will be shown, air speeds within the plume rising above the disc are also very low, typically under 1 m/s, making the air speed measurements practically impossible. Consequently, disc surface temperatures measured using contact thermocouples was found to be the only reliable method and these results were used to calculate average heat transfer coefficients, which will be compared with CFD results. As it will be shown later, some very useful but qualitative (only) indications of the flows were obtained using smoke generator.

3 CALCULATION OF AVERAGE HEAT TRANSFER COEFFICIENTS FROM MEASURED TEMPERATURES

As explained in the previous section, during the cooling period there is no heat input. Therefore, the energy dissipated during the time period t_1 to t_2 will be equal to the thermal energy loss from the disc. Consequently the average total heat transfer coefficient h_{tot} can be defined as:

$$h_{tot} = -\ln\left(\frac{T_{d2} - T_{\infty}}{T_{d1} - T_{\infty}}\right) \frac{m \cdot c_p}{A_w (t_2 - t_1)}, \quad (1)$$

where:

- T_{d2} is disc temperature at the time t_2 ;
- T_{d1} is disc temperature at the time t_1 ;
- T_{∞} is ambient temperature;
- m is disc mass;
- c_p is specific heat of disc material (grey iron);
- A_w is total disc wetted area.

The average coefficient of heat transfer due to radiation during the period $(t_2 - t_1)$ can be defined as:

$$h_{rad} = \varepsilon \cdot \sigma \left(\frac{T_d^4 - T_{\infty}^4}{T_d - T_{\infty}} \right) \frac{A_{rad}}{A_w}, \quad (2)$$

where:

- ε is disc surface emissivity;
- σ is Stefan-Boltzmann constant;
- A_{rad} is radiative heat dissipation disc area;
- T_d is average disc temperature during the period $(t_2 - t_1)$.

Accordingly, the average convective heat transfer coefficient, for the period $(t_2 - t_1)$, can be calculated as:

$$h_{conv} = h_{tot} - h_{rad}. \quad (3)$$

As the disc cools down, temperature will drop slower, hence keeping the same time periods $(t_2 - t_1)$, for calculating average heat dissipation coefficients may not be the best approach. It was found very useful to keep the temperature differences $(T_{d2} - T_{d1})$ constant for conducting

these calculations. Typically, temperature differences of around 20°C are considered most suitable, providing reliable disc surface temperatures and sufficiently short periods to account for highly non-linear influence of radiative heat losses. In order to determine disc surface emissivity, thermal camera (explained above) was used and the temperature was measured at the same time in the close proximity to the predefined points using contact thermocouples. After extensive surface mapping an average emissivity value was established for the entire disc surface. There were some variations between discs (which were taken into consideration when processing the data) but the overall average value was found to be $\varepsilon = 0.82$. It should be pointed out that disc surface was oxidised, covered in fine corrosion after repeated heating and cooling. There were no pads to polish the disc surface and contact/rubbing thermocouples covered only small area and caused little change to the surface emissivity in the contact paths with the disc (as the disc was rotating during heating period but the speeds and interface pressures were very low).

4 CFD MODELLING AND COMPARISON WITH EXPERIMENTAL RESULTS

CFD modelling for VW front and rear disc was conducted using CFX code [30].

4.1 CFD Mesh

Figs. 8a to 8d depict front ventilated disc model, with Fig. 8a showing the air domain, 8b and 8c surface mesh on the outboard and inboard side respectively. Mesh detail in the area of channel entrance at disc inner diameter is shown in Fig. 8d, where very fine mesh, with numerous small cells can be observed.

Figs. 9a and 9b shows rear solid disc, where the mesh did not require that many cells. Mesh statistics, for the two discs, is included in Table 3.

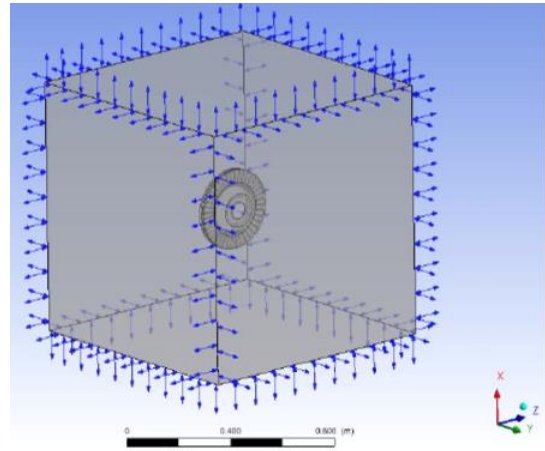


Fig. 8a. CFD Modelling of the ventilated disc: air domain

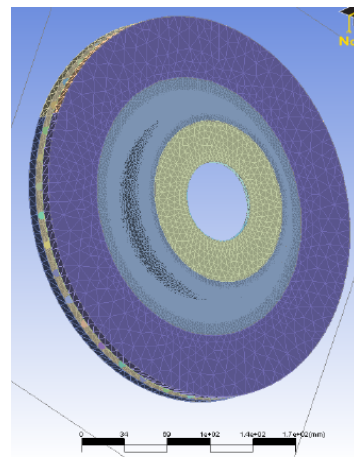


Fig. 8b. CFD Modelling of the ventilated disc: surface mesh (outboard)

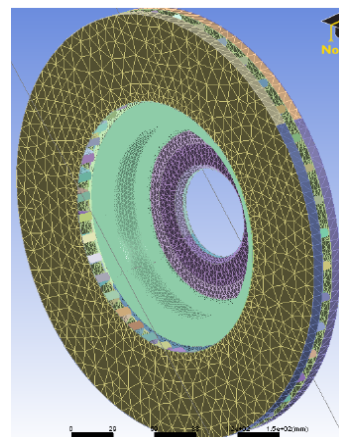


Fig. 8c. CFD Modelling of the ventilated disc: surface mesh (inboard)

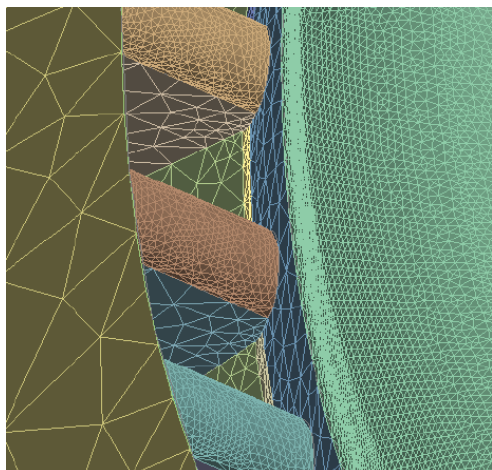


Fig. 8d. CFD Modelling of the ventilated disc: mesh detail

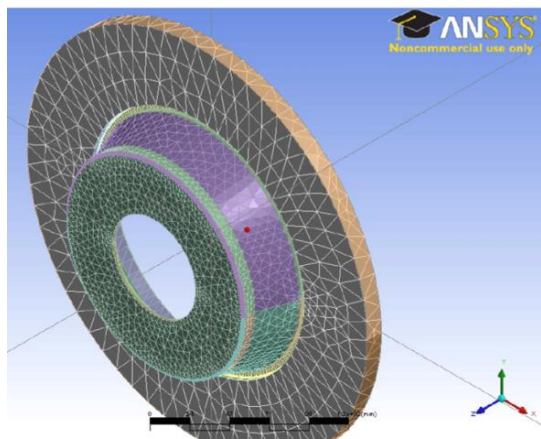


Fig. 9a. CFD Modelling of the solid disc: surface mesh

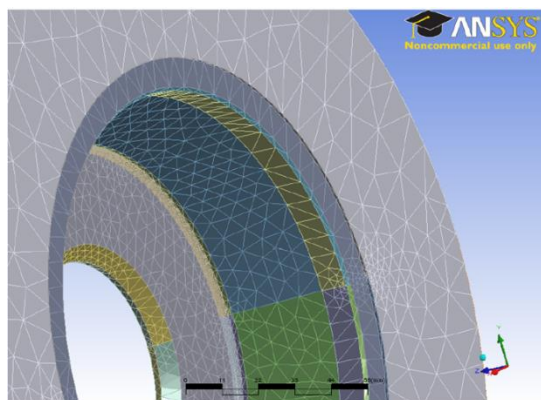


Fig. 9b. CFD Modelling of the solid disc: mesh detail

The total number of cells was over 12 million for the ventilated and over 3 million for the solid disc. It should be pointed out that such a fine

mesh was necessary for modelling air flow and heat transfer of stationary discs. Much lower number of cells was needed when modelling rotating disc or disc in a cross flow. $K-\varepsilon$ turbulence model was used for both discs and the results will be firstly presented alongside qualitative experimental investigations using smoke generator.

Table 3. CFD Mesh statistics

Characteristic	Ventilated disc (fine mesh)	Solid disc
Nodes (total)	3 295 654	857 655
Elements (total)	12 117 247	3 226 623
Of which:		
Tetrahedral	8 825 745	2 406 319
Pyramids	112	287
Prisms	3 291 390	820 017

4.2 Air Flow

Fig. 10a shows air velocity contours for the ventilated disc at 250 °C in the middle vertical plane (XZ, see Fig. 8a). It can be seen that the maximum velocity predicted is just over 0.9 m/s, therefore it was not possible to conduct experimental validation. In order to validate flow pattern, tests were conducted using smoke generator with neutral buoyancy smoke (generated from special oil), with the fine probe releasing the smoke in various areas in the proximity to the disc. Fig. 10b shows the plume rising from the disc faces and channels, which closely resembles the CFD predictions displayed in Fig. 10a. It should be pointed out that, unfortunately, the disc could not be heated to 250°, the temperature used for CFD modelling.

The flow air patterns (such as Fig. 10b) are very difficult to photograph and obtain clear flow indications. The best approach established was to take videos and then play them frame by frame and select the clearest pictures with the highest contrast. This approach inevitably reduced picture resolution, with the disc cooling down during filming. The light also played an important part in taking useful images - too much or too little light made the smoke practically invisible or air plume direction difficult to understand. As expected, the cooling is most effective in the upper side of the disc, and least effective in the channels which are in the horizontal position.

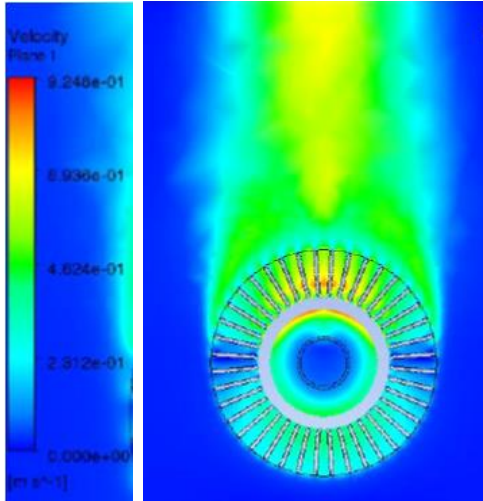


Fig. 10a. Ventilated disc: CFD air velocities



Fig. 10b. Ventilated disc: flow (smoke) pattern using smoke generator

Fig. 11a shows air velocity contours in the vertical plane YZ running through the disc axis, with 11b showing horizontal plane XY, again running through the disc axis. It can be noticed that upwards air flow in the swan neck area, at disc inner diameter, blocks air entry into the ventilation channels. This phenomenon (effect) diminishes with drop in disc temperatures. As a result, convective cooling does not drop as drastically as probably expected with disc cooling, owing to

(proportionally) more air flow going through ventilation channels at lower disc temperatures.

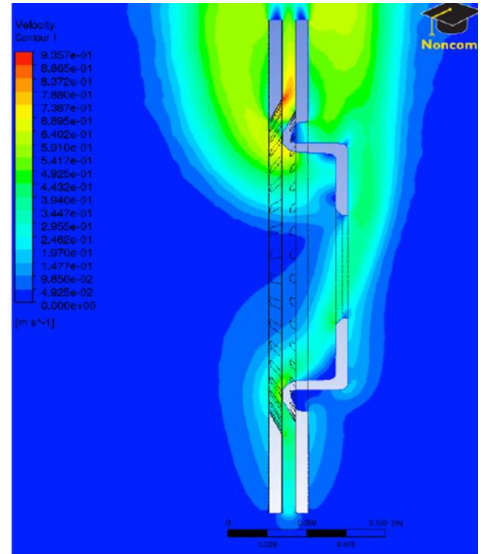


Fig. 11a. Ventilated disc predicted air velocity contours at 250°C: YZ plane

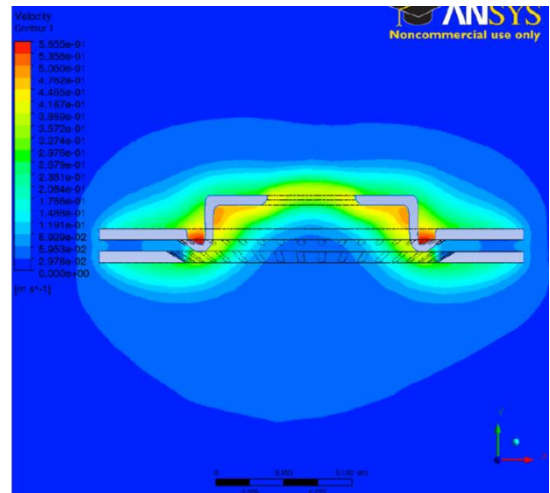


Fig. 11b. Ventilated disc predicted air velocity contours at 250°C: XY plane

Figs. 12a and 12b shows the solid disc. Again, CFD analyses were performed for 250°C and experiments at 150°C due to the limitation of the heating system. CFD air velocities are shown in the line form (Fig. 12a) and all indications are that the flow pattern matches very well with the visualisation using smoke generator shown in Fig. 12b. The maximum air speeds predicted were just over 0.6 m/s, more than one disc diameter above

the disc, in the middle plane. Unfortunately, this value is very low and could not be experimentally verified but the smoke rising above the disc (Fig. 12b) clearly indicates the same pattern and position of the highest speed.

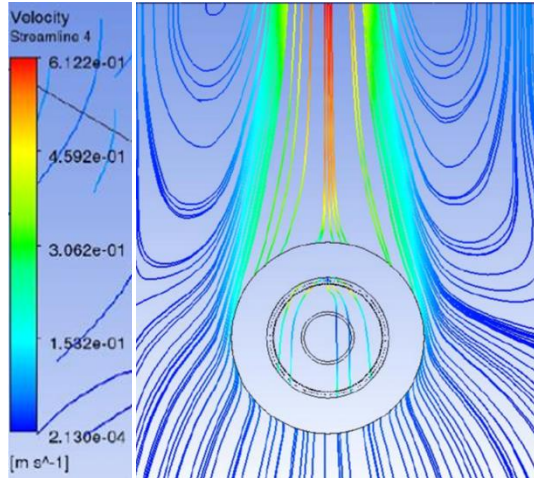


Fig. 12a. Solid disc: CFD air velocities

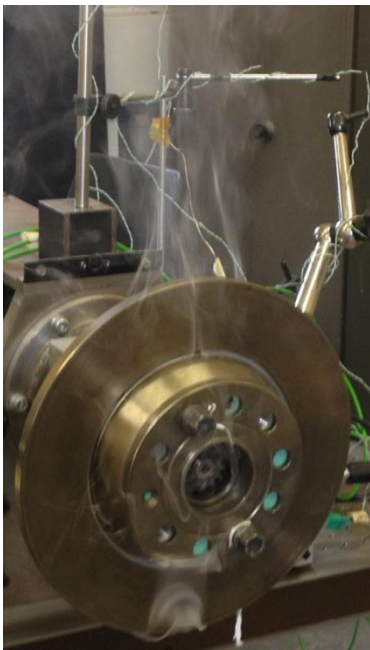


Fig. 12b. Solid disc: Flow (smoke) pattern using smoke generator

4.3 Air temperatures

Despite not being able to accurately measure air temperatures, it is useful to look at the CFD results shown in Fig. 13 for the ventilated

(13a) and solid (13b) discs at 250°C (note the air temperature is shown in K). Air temperature seems to rapidly drop after rising above the disc. The plume is also relatively narrow. That probably best explains why the efforts in measuring air temperature was not successful in this case. In one study [1] air temperatures were successfully measured but for much larger and heavier commercial vehicle brake discs heated to higher temperatures. The air temperatures shown in Figs. 13a and 13b match well with the air speed and flow patterns shown in Figs. 10a to 12b.

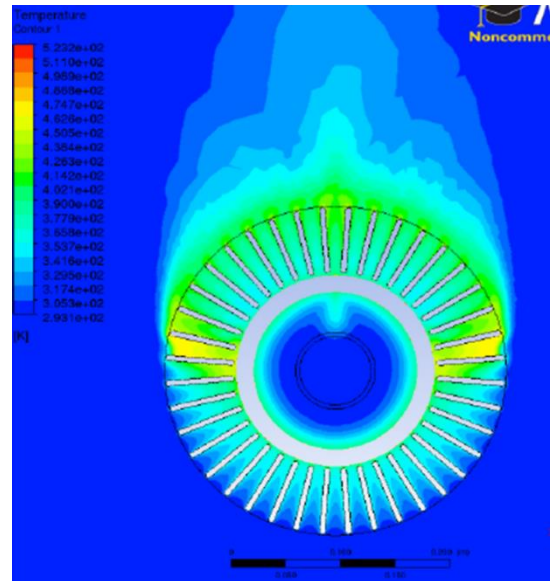


Fig. 13a. Air temperature contour in XZ plane for discs at 250°C: Ventilated disc

4.4 Heat Transfer Coefficients

CFD analyses also enabled predictions of the local and average convective heat transfer coefficients over the disc surfaces, with Fig. 14 showing the ventilated and Fig. 15 solid disc. For both designs it is clear that convective heat dissipation is more effective from the upper part of the disc, as it would be expected. On the outboard side of the disc the effect of the hub (top hat) can also be observed. The flow is blocked and there is a reduction of the convective cooling in the middle of the disc, above the hub. However, this effect is not present on the inboard side of the disc friction faces. Maximum values of the heat transfer coefficient reach approx. 14.8 W/m²K for the ventilated disc (Fig. 14) and 8.2 W/m²K for the

solid disc (Fig. 15) but these values of the convective heat transfer coefficients are limited to very small areas with no practical significance for disc cooling. For both designs, the highest values covering larger disc areas are around $5 \text{ W/m}^2\text{K}$. CFD analyses enabled automatic calculations of average values for the convective heat dissipation coefficients, from the distributions shown in Figs. 14 and 15.

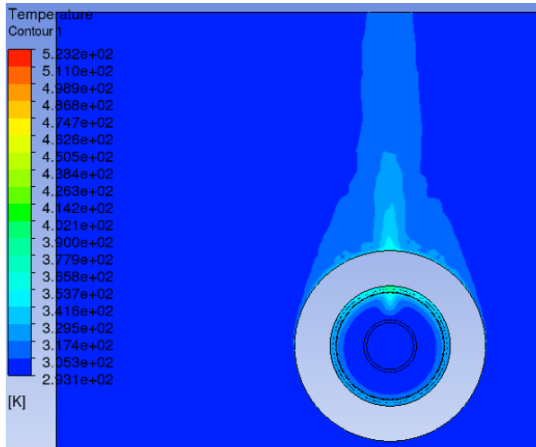


Fig. 13b. Air temperature contour in XZ plane for discs at 250°C: Solid disc

Experimental investigations enabled only the extractions of average convective heat dissipation coefficients, from the average cooling curves (measured surface temperatures during disc cooling). The measurements of disc surface temperatures proved to be very repeatable and reliable. The procedure for calculating average convective heat transfer coefficients from cooling curves was explained earlier on, which now enables for these values to be compared with CFD results. To cover the temperature range, CFD analyses had to be repeated for lower temperatures. The comparisons presented in Figs. 16 and 17 for ventilated and solid discs respectively, show quite interesting phenomena. For the ventilated disc (Fig. 16), the average convective heat transfer coefficients calculated from the measured cooling curves have higher values than CFD predictions. The gradient is also steeper, the cooling is becoming more effective with increase in disc temperature. Unfortunately, with the heating system available it was not possible to heat the disc to higher experimental temperatures but for disc at around 100°C , the experimental values are about

40% higher. For the solid disc (Fig. 17) experimental and CFD values of the convective heat transfer coefficient are much closer. Experimental values are again higher but only by about 8%. Though the experiments and CFD analyses were conducted for the same discs and nominal conditions, there were differences in 'holding' the discs, as the discs were completely free standing in still air in CFD analyses (see Figs. 8a and 9a), whereas they were mounted to the hub flange and in proximity to the upright in experiments (see Fig. 3a).

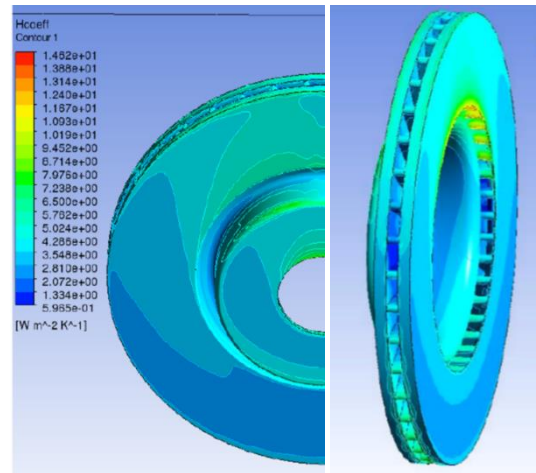


Fig. 14. Predicted convective heat transfer coefficient distribution for ventilated disc

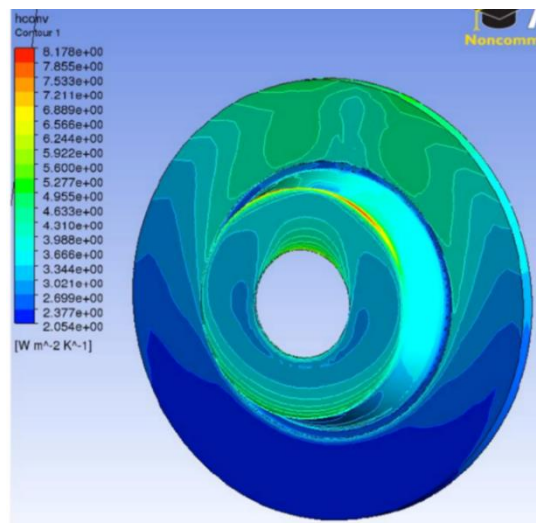


Fig. 15. Predicted convective heat transfer coefficient distribution for solid disc

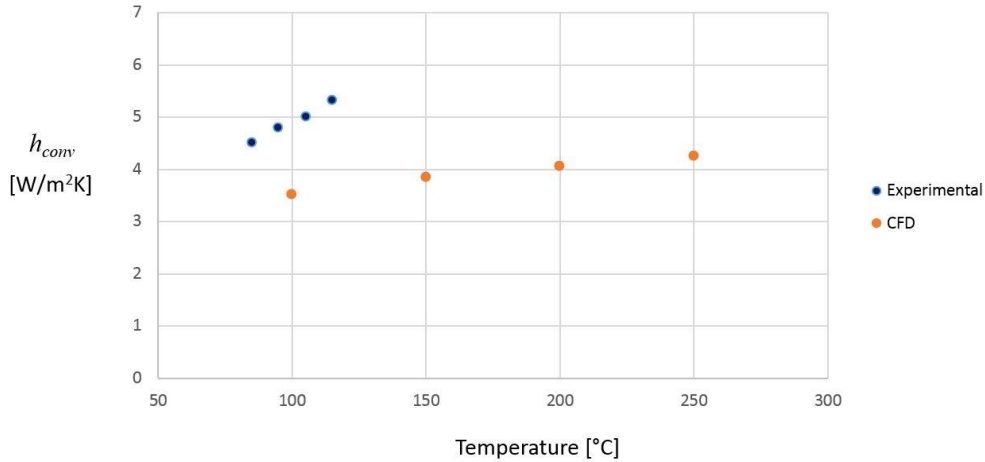


Fig. 16. Ventilated disc: Experimental and CFD average convective heat transfer coefficients

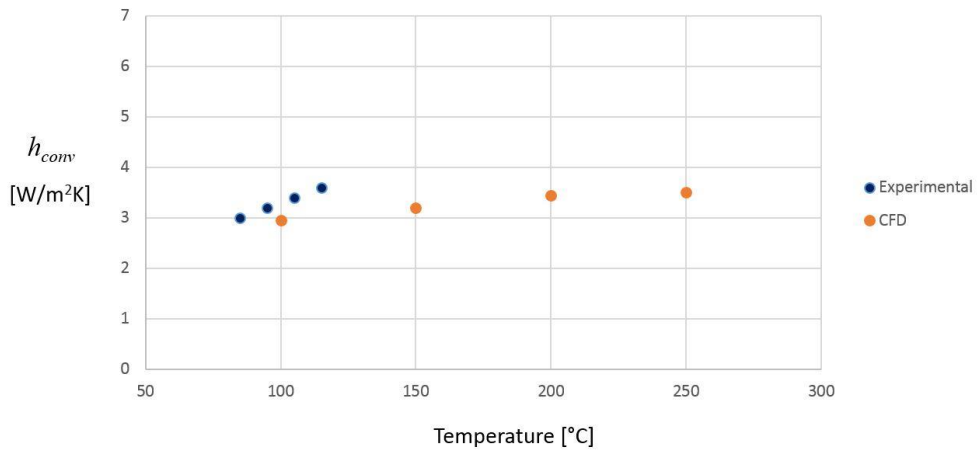


Fig. 17. Solid disc: Experimental and CFD average convective heat transfer coefficients

Table 4. Measured average convective heat transfer coefficients for four designs studied

Ref. Fig. 1	Disc design	h_{conv} [W/m²K]			
		Temperature range [°C]			
		120 - 110	110 - 100	100 - 90	90 - 80
a)	Ventilated with radial vanes	5.3	5.0	4.8	4.5
b)	Solid	3.6	3.4	3.2	3.0
c)	Ventilated with curved vanes	4.2	3.8	3.7	3.5
d)	Ventilated with curved vanes; cross drilled	4.4	4.1	3.7	3.5

5 DISCUSSION

Conducted CFD analyses under-predicted the values of the convective heat transfer coefficients. This was particularly the case for the ventilated disc, which has much more complex flow patterns. It was also established that ventilated disc has higher values of the convective

heat transfer coefficient, with this design also having much higher total wetted area. The combined effects will considerably increase convective dissipation but higher thermal capacity of this disc must be also considered. Ventilated disc has approximately 1.8 times higher wetted area and 2.9 times higher mass. Overall, the

indications are that the two designs would cool at relatively similar rate in still air, from the same initial temperatures. This might change on the vehicle but generally is a good sign of maintaining relatively comparable temperatures of the front and rear brakes.

In addition to the VW Passat front and rear discs, it is interesting to present measured values of the two Lotus Elise S2 disc designs. As no CFD analyses were conducted for these discs, only experimental values are presented in Table 4 in order to compare them with those of VW Passat discs.

The overall h_{conv} values (Table 4) indicate that the disc with radial vanes (VW Passat front) has the highest cooling rates and the solid disc (VW Passat rear) the lowest. Curved vanes help in increasing air flow and convective cooling of rotating discs but in stationary conditions curved vanes trap the air, preventing the buoyant flow upwards. It is also interesting to see (Table 4) that cross drilling has practically no influence at lower temperatures up to about 100°C but at higher temperatures there is a measurable improvement of about 5% at 120°C. CFD analyses were not performed for curved vane discs but some of the following photographs effectively illustrates air flow in stationary cooling.

Fig. 18 effectively illustrates the problem with stationary cooling of the curved vane discs. At the mid horizontal plane, at the end where the flow channels (and vanes) point upwards (18a), the upwards flow is reasonable and seems very steady. The smoke is rising smoothly. However, at diametrically opposite end (18b and c) where the vanes point downwards, there is obvious slowing down of the flow and chocking. The smoke is stagnant. The flow through the bottom and top of the ventilation channels is not particularly good either.

Fig. 19 presents cross drilled disc, showing a similar flow problems to the standard, non-drilled disc (Fig. 18). At the mid horizontal plane, at the end where the flow channels (and vanes) point upwards (19a), the flow is reasonable and seems very steady, similarly to the non-drilled disc (Fig. 18a). However, at the diametrically opposite end (19b and c), there is obvious obstruction and chocking. To a certain degree the holes drilled through friction faces help the flow and in Fig. 19c there is a clear view of the smoke rising upwards through the cross drilled holes. It is reasonable to

assume that in some areas the holes will also provide air entry, helping the overall cooling. The effects are expected to be more pronounced with increased buoyancy, and the values in Table 4 prove that, with the cross drilled disc showing superior cooling characteristics at higher temperatures (in comparison to the standard disc). The flow through the bottom and top of the ventilation channels can be also marginally helped with cross drilling.

6 CONCLUSIONS

Experimental investigation of the heat dissipation from stationary discs was successful in ensuring repeatable and accurate measurement and prediction of the total, convective and radiative heat dissipation coefficients. The values compare favourably with CFD analyses, though the differences are somewhat pronounced for the ventilated discs. The speeds of the hot air rising above the disc are far too low and flow pattern narrow and relatively irregular, making the validation of air speeds and air temperatures practically impossible. However, the use of smoke generator (with neutral buoyancy smoke) and suitable probe was very useful in qualitatively validating the flow patterns.

Convective heat transfer coefficients increase with temperature but the values are very low, typically between 3 and 5 W/m²K for the disc designs and temperature range analysed. As expected, out of the four designs studied, the disc with radial vanes has highest convective heat dissipation coefficient and the solid disc the lowest. The reduction is about 30%, with the disc with curved vanes values being about 20% lower than for the disc with radial vanes.

Low values of convective heat transfer coefficients indicate low dissipated energy (heat), in particular for the solid disc. Consequently, cooling times are very long and the contribution of the other two heat dissipation modes, conduction and radiation higher. At high disc temperatures (>400°C), radiative losses in stationary conditions can be an order of the magnitude higher than convective.

When installed on the vehicle, with the addition of the caliper assembly, wheel, mudguard and dust shield, the cooling of brake discs is likely to be even further reduced. Future work is concentrated in addressing this challenge in two

ways, by improving CFD modelling and equipping the Thermal Spin Rig with induction heater to heat

the disc much more rapidly and to much higher temperatures.

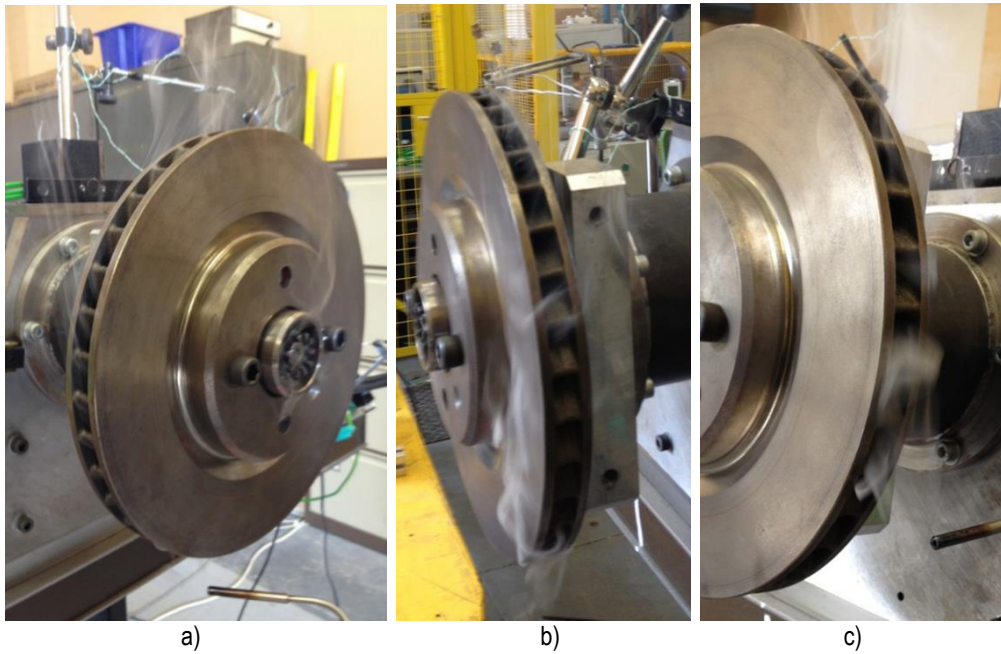


Fig. 18. Curved vane standard disc smoke tests:
(a) Flow channels pointing upwards; (b) and (c) Flow channels pointing downwards

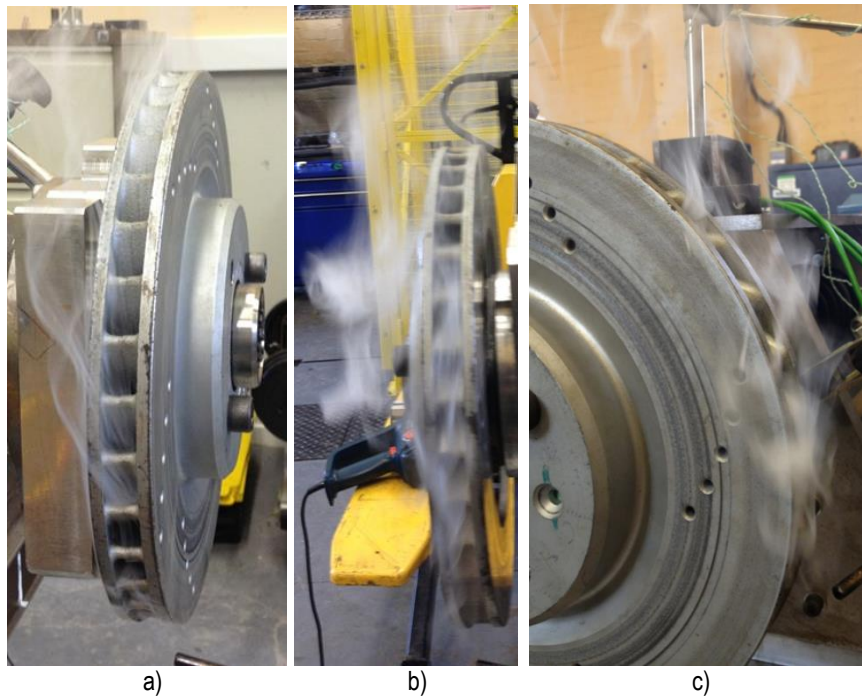


Fig. 19. Curved vane cross drilled disc smoke tests:
(a) Flow channels pointing upwards; (b) and (c) Flow channels pointing downwards

Cross drilling of the disc with curved vanes seems to only marginally improve static cooling, predominantly at higher temperatures.

7 ACKNOWLEDGEMENTS

Some of the presented results are part of a project financed by the Serbian Ministry of Education, Science and Technological Development (Project TR 35045 - "Scientific-Technological Support to Enhancing the Safety of Special Road and Rail Vehicles", project leader - prof. dr Vladimir Popović).

8 NOMENCLATURES

A_w	[m ²]	total disc wetted area
A_{rad}	[m ²]	radiative heat dissipation disc area
c_p	[J/kgK]	specific heat of disc material (grey iron)
h_{tot}	[W/m ² K]	total average heat transfer coefficient
h_{conv}	[W/m ² K]	average convective heat transfer coefficient
h_{rad}	[W/m ² K]	average radiative heat transfer coefficient
m	[kg]	disc mass
T_d	[K]	average disc temperature during time period ($t_2 - t_1$)
T_{d1}	[K]	disc temperature at the time t_1
T_{d2}	[K]	disc temperature at the time t
∞	[K]	ambient air temperature
t	[s]	time
ε	[-]	disc surface emissivity
σ	[W/m ² K ²]	Stefan-Boltzmann constant ($5.67 \cdot 10^{-8}$)

9 REFERENCES

- [1] Stevens, K. (2013). *An Investigation into Heat Dissipation from a Stationary Commercial Vehicle Brake Disc in Parked Conditions (EngD Thesis)*. Cranfield University.
- [2] Wagner, C. (1948). Heat transfer from a rotating disk to ambient air. *Journal of Applied Physics*, vol. 19, no. 9, p. 837-839.
- [3] Cobb, E.C., Saunders, O.A. (1956). Heat transfer from a rotating disk. *Proceedings of the Royal Society A: Mathematical, Physical and Engineering Sciences*, vol. 236, no. 1206, p. 343-351.
- [4] Richardson, P.D., Saunders, O.A. (1963). Studies of flow and heat transfer associated with a rotating disc. *Journal of Mechanical Engineering Science*, vol. 5, no. 4, p. 336-342.
- [5] Newcomb, T.P. (1959). Transient temperatures attained in disk brakes. *British Journal of Applied Physics*, vol. 10, no. 7, p. 339-340.
- [6] Newcomb, T.P., Spurr, R.T. (1967). *Braking of Road Vehicles*. Chapman & Hall, London.
- [7] Grkić, A., Mikluc, D., Muždeka, S., Arsenić, Ž., Duboka, Č. (2015). A Model for the estimation of brake interface temperature. *Strojniški vestnik - Journal of Mechanical Engineering*, vol. 61, no. 6, p. 392-398.
- [8] Noyes, R.N., Vickers, P.T. (1969). Prediction of surface temperatures in passenger car disc brakes, SAE Technical Paper no. 690457.
- [9] Morgan, S., Dennis, R.W. (1972). A theoretical prediction of disc brake temperatures and a comparison with experimental data, SAE Technical Paper no. 720090.
- [10] Limpert, R. (1975). Cooling analysis of disc brake rotors, SAE Technical Paper no. 751014.
- [11] Sisson, A.E. (1978). Thermal analysis of vented brake rotors, SAE Technical Paper no. 780352.
- [12] Daudi, A.R. (1999). 72 curved fins and air director idea increase airflow through brake rotors, SAE Paper Technical Paper no. 1999-01-0140.
- [13] Galindo-Lopez, C.H., Tirovic, M. (2008). Understanding and improving the convective cooling of brake discs with radial vanes. *Proceedings of the Institution of Mechanical Engineers, Part D: Journal of Automobile Engineering*, vol. 222, no. 7, p. 1211-1229.
- [14] Galindo-Lopez, C. H., Tirovic, M. (2013). Maximizing heat dissipation from ventilated wheel-hub-mounted railway brake discs. *Proceedings of the Institution of Mechanical Engineers, Part F: Journal of Rail and Rapid Transit*, vol. 227, no. 3, p. 269-285.
- [15] Pevec, M., Potrc, I., Bombek, G., Vranesevic, D. (2012). Prediction of the cooling factors of a vehicle brake disc and its influence on the results of a thermal numerical simulation.

- International Journal of Automotive Technology*, vol. 13, no. 5, p. 725-733.
- [16] Son, J.K., Jung, Y-S., Jeon, H-H. (2018). Optimization analysis and design of brake cooling system. *EuroBrake 2018 Conference Proceedings*, paper EB2018-SVM-003.
- [17] Stevens, K., Tirovic, M. (2018). Heat dissipation from a stationary brake disc, Part 1: Analytical modelling and experimental investigations. *Proceedings of the Institution of Mechanical Engineers, Part C: J Mechanical Engineering Science*, vol. 232, no. 9, p. 1707-1733.
- [18] Tirovic, M., Stevens, K. (2018). Heat dissipation from a stationary brake disc, Part 2: CFD modelling and experimental validations. *Proceedings of the Institution of Mechanical Engineers, Part C: J Mechanical Engineering Science*, vol. 232, no. 10, p. 1898-1924.
- [19] McAdams, W.H. (1954). *Heat Transfer*. McGraw-Hill, New York City.
- [20] Morgan, V.T. (1975). The overall convective heat transfer from smooth circular cylinders. *Advances In Heat Transfer*, vol. 11, p. 199-264.
- [21] Churchill, S.W., Chu, H.H.S. (1975). Correlating equations for laminar and turbulent free convection from a horizontal cylinder. *International Journal of Heat Mass Transfer*, vol. 18, no. 9, p. 1049-1053.
- [22] Necati Özisik, M. (1989). *Heat Transfer: A Basic Approach*. McGraw-Hill, New York City.
- [23] Tirovic, M., Voller, G.P. (2005). Interface pressure distributions and thermal contact resistance of a bolted joint. *Proceedings of the Royal Society A: Mathematical, Physical and Engineering Sciences*, vol. 461, no. 2060, p. 2339-2354.
- [24] Teimourimanesh, S., Vernersson, T., Lunden, R. (2014). Modelling of temperatures during railway tread braking: Influence of contact conditions and rail cooling effect. *Proceedings of the Institution of Mechanical Engineers, Part F: Journal of Rail and Rapid Transit*, vol. 228, no. 1, p. 93-109.
- [25] Eisengräber, R., Grochowicz, J., Schuster, M., Augsburg, K., Koch, L. (1999). Comparison of different methods for the determination of the friction temperature of disc brakes, SAE Technical Paper no. 1999-01-0138.
- [26] Dufrenoy, P., Berte, E., Witz, J-F., Desplanques, Y. (2018). A new camera for quantitative measurements of temperature and emissivity during braking. *EuroBrake 2018 Conference Proceedings*, paper EB2018-VDT-033.
- [27] Grieve, D.G., Barton, D.C., Crolla, D.A., Buckingham, J.T. (1998). Design of a lightweight automotive brake disc using finite element and Taguchi techniques. *Proceedings of the Institution of Mechanical Engineers, Part D: Journal of Automobile Engineering*, vol. 212, no. 4, p. 245-254.
- [28] Tang, J., Bryant, D., Qi, H. (2018). Experimental investigation of the dynamic thermal deformation and judder of a ventilated disc brake. *EuroBrake 2018 Conference Proceedings*, paper EB2018-FBR-002.
- [29] Topouris, S. (2017). *Design and Optimisation of a High Performance Lightweight Monoblock Cast Iron Brake Disc (PhD Thesis)*. Cranfield University.
- [30] Olphe-Galliard, M. (2011). *Study of Thermodynamics and Fluid Mechanics Involved in the Cooling of Brake Discs (MSc Thesis)*. Cranfield University.